Article

Modeling of Sediment Transportation in Ichkeul Lake for the Estimation of the Influence of the Constructions of the Reservoirs in the Upper Streams

Mitsuteru Irie [1],* , **Hirotoshi Kotegawa [2]**, **Atsushi Kawachi [3]**, **Hajel Ouni [4]** and **Jamila Tarhouni [4]**

1   Faculty of Engineering, University of Miyazaki, Miyazaki 889-2192, Japan
2   Maeda Construction Co., Ltd., Tokyo 102-8151, Japan; kotegawa.h@jcity.maeda.co.jp
3   Token C.E.E. Consultant, Tokyo 170-0004, Japan; kawachi-a@tokencon.co.jp
4   Institut National Agronomique de Tunisie, Université de Carthage, Tunis 1082, Tunisia;
     ouni_hajer@hotmail.fr (H.O.); elmaainat@yahoo.fr (J.T.)
*   Correspondence: irie.mitsuteru.p2@cc.miyazaki-u.ac.jp; Tel.: +81-2958-7341

Abstract: Rich ecosystems such as estuaries and brackish lakes are vulnerable to the effects of human activities and are prone to environmental changes. In particular, the salt environment, which is the backbone of the environment, might be affected not only by direct modifications such as dredging but also in ways that were not initially envisioned. Ichkeul Lake, located in the northern part of Tunisia, is a shallow brackish lake registered as a UNESCO World Natural Heritage Site. The construction of reservoirs upstream of the inflowing river in the 1980s reduced the amount of freshwater inflow. That only had been thought to be the cause of the increase in salinity in Ishkeul Lake. On the other hand, the sedimentation in the reservoirs upstream was remarkable, and the supply of sediment from the reservoirs upstream to the Ichkeul Lake was stopped. Changes in sediment outflow may have reduced lakebed altitude and enhanced seawater intrusion. However, the environmental protection measures for the lake so far have focused only on improving the water budget and have not been quantitatively evaluated for sediment transportation. In this study, we first estimated the water budget of the lake. Then the re-suspension by wind disturbance in the lake was estimated from the correlation with the wind speed based on laboratory experiments and field measurements. The outflow of the sediment estimated with these two models was compared with the sediment volume trapped in the upstream reservoirs that would have flowed into the lake if there had been no construction of the dams. Based on this, we evaluated whether the lake is currently erosive or cumulative. As a result, the estimated annual outflow of sediment to the sea was 4300 tons/year. It was estimated that the construction of the reservoirs upstream changed the trend of lakebed height from accumulation to erosion.

Keywords: sediment transportation; resuspension; brackish lake; water budget; SWAT

1. Introduction

In brackish lakes and estuaries, where freshwater and seawater are mixed, the fluctuation of salinity supports the precious habitat of endemic species migrating from both sea and freshwater areas. Rich ecosystems established under such geographical and hydrological conditions are susceptible to the influence of human activities, and international conservation actions such as the Ramsar Convention are required. Typical examples are dredging for navigation or flood control which have environmental impacts due to the changes in salinity conditions. Miller [1] evaluated the salinity response to dredging under different forcing regimes for a 75-km segment of the flood-prone Vermilion River located in coastal Louisiana, USA. Yuan & Zhu [2] estimated the influences of channel deepening and widening on the tidal and nontidal circulations of Tampa Bay, based on the numerical three-dimensional ocean model. They found that the tidal range increased, and the tidal

phase decreased from the mouth to the head of the bay after deepening and widening of the channel. van Dijk et al. [3] showed how dredging changes the natural development of estuaries through a combination of experiments in the laboratory and a numerical simulation. They quantified the effect of the increase of shipping draft and sea-level rise on estuary morphodynamics and habitat suitability. Dias et al. [4] clarified the impact of the general deepening of the lagoon, such as the increase of tidal currents and salt intrusion through field observations and numerical simulations.

In addition to the environmental impacts of such direct morphological changes, there are some cases in which the change of the sediment supply through the erosion process upstream governs the river morphology and shoreline landscape [5]. Sediment supply to downstream rivers worldwide has been dramatically reduced due to dams, especially in the more recent decades. The rapid flow from dams flashes fine material on the riverbeds and deepens the channels downstream. Kondolf et al. [6] argued that hydropower dams trap all bedload and a huge amount of suspended load, releasing sediment-starved flow downstream. The closure of Aswan High Dam in the Nile River has trapped almost all of the sediment from reaching the Nile River delta [7]. Manwan Dam on the Mekong River has trapped about 50% of the sediment budget of the river [8]. The development of water resources in the upper catchment needs to be considered as a factor of environmental impacts on the estuary zone.

Ichkeul Lake, located in the northern part of Tunisia, is a shallow brackish lake registered as a UNESCO World Natural Heritage Site (Figure 1). After the construction of the dams upstream: Joumine in 1983, Ghezala in 1984, and Sejnane in 1994, an important fraction of the flow was diverted towards agriculture and domestic uses. Due to the decrease of the freshwater inflow in rainy winter from the upper stream, the average water level of the lake was lowered and the duration and volume of reverse flow in the dry season from the sea became longer and larger. The increase in the salinity of the lake affected the dominant aquatic plants and destroyed the habitat of migratory birds. The park was listed on the World Heritage in Danger List from 1996 to 2006.

On the other hand, the sedimentations in the upstream reservoirs are very severe. Irie et al. [9] estimated the total sedimentation volume in the two large reservoirs upstream based on bathymetric surveys. The annual average accumulation volume of the sediment in total was 570,000 tons/year. In addition, due to the structures of the dam bodies and the grain size characteristics of the solid matter, bottom density currents occur in the reservoirs. During that period, clear water overflows from the spillway of a dam to the lake in contrast to the runoff which has a concentration higher than 1000 ppm into the reservoir. A large part of the solid matter transported from the upper catchment is trapped in the reservoirs [10]. On the other hand, in winter, the west wind lifts the bed material and the forward flow from the lake to the sea continues. As a result, it is supposed that the height of the lakebed decreases due to the imbalance of sediment, and parallelly, the lower lake water level enhances seawater intrusion. It is obvious that the decrease in freshwater inflow due to the construction of the reservoirs was a major factor in the salinity environment of the lake, but such changes in the budget of sediment transportation are also related to changes in the salinity environment. Since the focus of environmental conservation activities on the lake has been only to improve the water budget so far, the sediment budget has not been sufficiently evaluated quantitatively.

This study tried to evaluate the sediment outflow based on the calculation of the water budget of the lake and modeling the resuspension process from the observed wind data. The Soil & Water Assessment Tool (SWAT) model was applied to the upper catchment for the estimation of the water inflow to the lake. The outflow in winter from the lake to the sea was estimated using the hydraulic calculation with the gradient and width of the connecting channel. We assumed that resuspension occurs uniformly in a horizontal and vertical direction in the lake and that the concentration of the outflowing water was the same as that in the lake. The influence of the construction of the reservoirs on the budget of the sediment was discussed using a comparison of the budgets of the

sediment between the sediment outflow from the lake and the sedimentation in the reservoirs upstream.
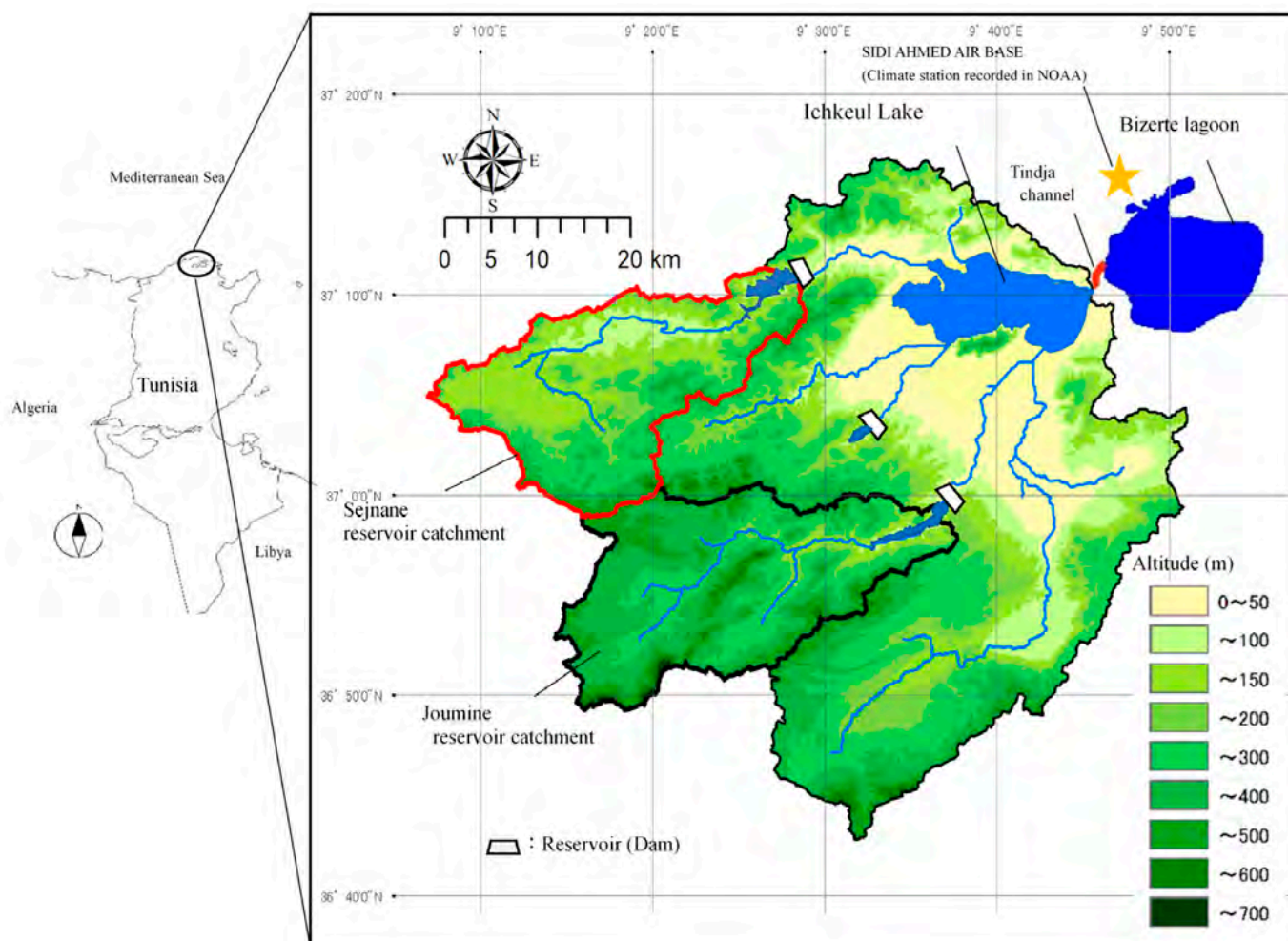

Figure 1. Catchments of Ichkeul Lake.

2. Materials and Methods

2.1. Study Site

Ichkeul Lake is a very shallow brackish lake with an average depth of about 2 m and an area of about 88 km^2 (Figure 2). Several rivers flow into the lake, and the total catchment area at the eastern end of the Atlas Mountains is about 2132 km^2. The average annual rainfall is about 600 mm. It is an important stop for migratory birds traveling from Central Europe and Holland. Four migratory species: greylag goose, widgeon, filigule pochard, and coot live and nest on Ichkeul Lake's wealth. Hence, Ichkeul is an internationally important site for these species. The birds' stopover provides habitat and food thanks to the two major aquatic plants characterizing Ichkeul Lake: Potamogeton pectinatus and Ruppia cirrhosa. The Potamogeton were distributed in lower salinity conditions (almost 7–9 PSU), while the Ruppia were in high-salinity conditions and exist on the bottom and in surface water [such as 9–11 practical salinity units (PSU)]. The Ruppia distribution area is spreading in a more southerly direction than that found in previous work [11]. In other words, a slight change in salinity conditions can significantly change the vegetation distribution.
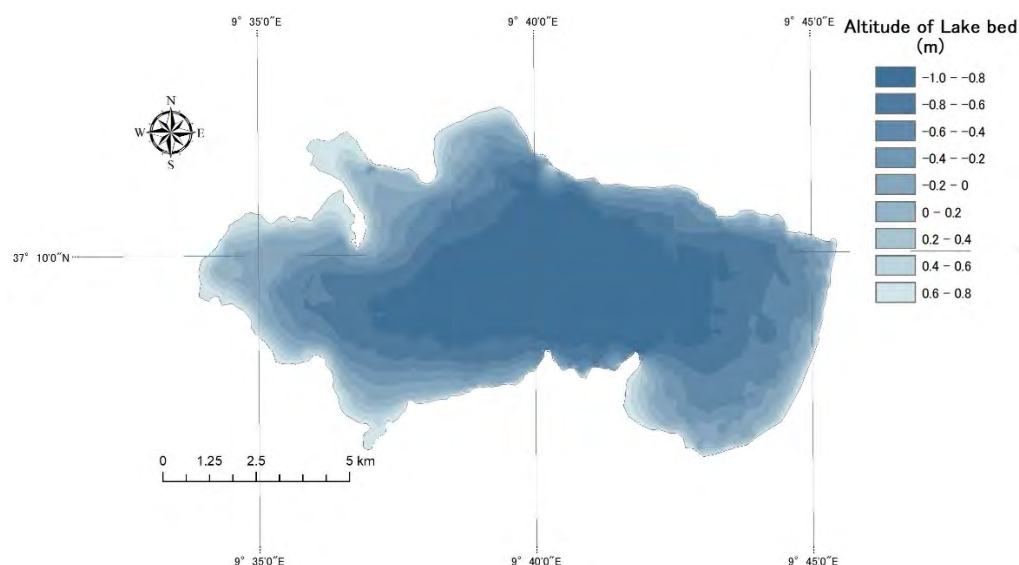
Figure 2. Bathymetry of Ichkeul Lake.

The climate of the site is the typical Mediterranean climate system. In the summer dry season, the lake water level drops due to little freshwater inflows, while the seawater flows into Lake Ichkeul from Bizerte Lagoon through the Tindja Canal (red line in Figure 1). Bizerte region, where Ichkeul Lake is located, is known for its strong winds, ranging from 5 to 9 m/s, but capable of reaching 15 m/s [12]. The most frequent winds blow from the W–NW. During spring and summer, wind speeds are relatively constant, while they are highly variable in autumn and winter. The strong wind in winter induces high turbidity in the lake water. Hajer et al. identified the spatial distribution of a water turbidity index, an indicator of the TSM with multi-date MODIS images. The relationship between the wind conditions and the resuspension from the lakebed was clarified [13]. The critical wind speed inducing resuspension in the lake was 2.8 m/sec. Such strong wind blows from the west in rainy winter when the lake water level is higher than the seawater level. The solid matter resuspended by the wind is outflowing with the forward flow in the connected channel.

Bizerte Lagoon is so deep (ave. 7 m, Mmax. 12 m) [14] that it is unlikely to be resuspended by the wind. In addition, the strong wind does not blow in the summer when the reverse flow to the lake occurs. Therefore, the transportation of solid matter in summer is less in Ichkeul lake. In the winter rainy season, the flow in Tinja channel is forward from the lake to the lagoon, due to the higher water level of the lake with the freshwater supply from the upper catchment area. At the same time, westerlies blow strongly in winter, causing resuspension of bottom material [15]. Therefore, the solid matter outflow from the lake to the lagoon occurs in winter [16], as illustrated in Figure 3.

Before the reservoirs were constructed, the budget of the solid matter in the lake was in equilibrium with the supply transported by the freshwater inflows from upstream and the forward outflow through the channel in winter. However, after the construction of the reservoirs, the solid matter inflows were trapped by the reservoirs as sediments in the reservoirs. Finally, the budget of solid matter was lost. The level of the lakebed decreased as a result of the excessive outflow. It is considered that the lake water level also dropped parallelly, causing the lake water level to be lower than sea-level for a longer period.

The results of a sedimentation survey conducted in 2010 at the reservoirs upstream of the lake [17], show that 17.8 million m^3 of sediment was deposited in the reservoir. If the accumulated sediment was deposited on the entire bed of the lake (an area of about 88 km^2), the thickness would be about 20 cm.
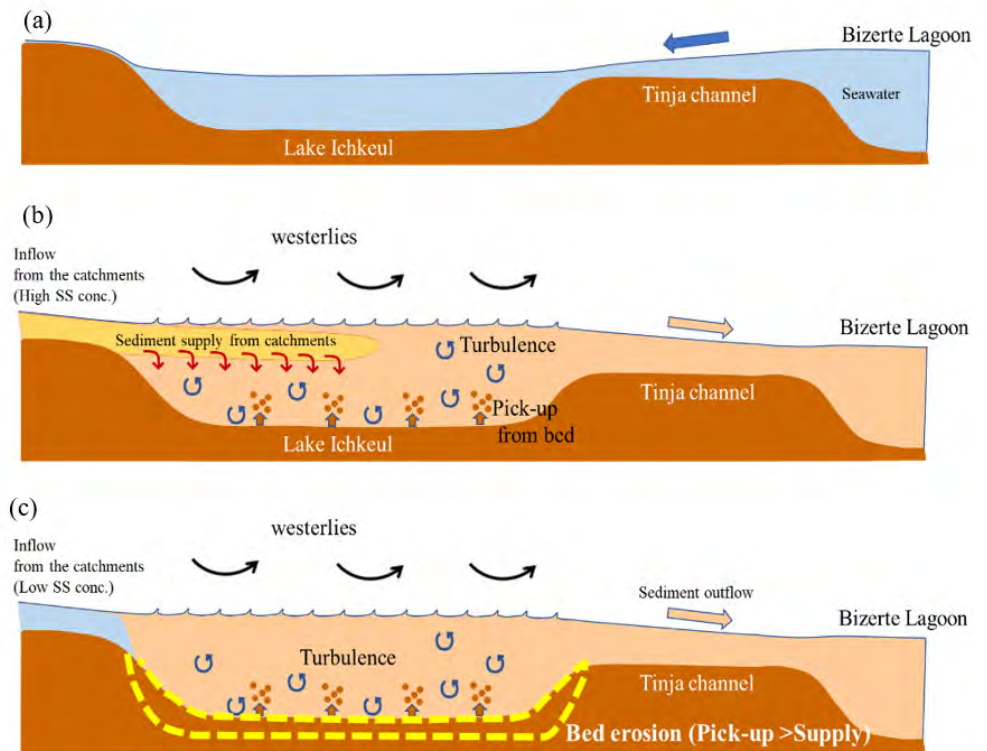
Figure 3. Schematic images of seawater intrusion and transportation of sediment in Ichkeul Lake and typical images of the water surface in summer and winter. (**a**) Dry season in summer (Lake < Lagoon: seawater intrusion). (**b**) Rainy season in winter (Lake > Lagoon: resuspension of bed material) without dams. (**c**) Rainy season in winter with dams (Sediment supply = 0).

2.2. Estimation of the Water Budget of the Lake

The lake water level has been observed for a long time by the local government in Ichkeul Lake, but the inflow and outflow have not been continuously observed. The water budget in the lake is estimated based on the following formula:

$$Q_{in} - Q_{out} - evapo. = \pm \Delta V \tag{1}$$

where Q_{in} is the total inflow from the catchments, Q_{out} is the outflow from the lake to Bizerte Lagoon, *evapo.* is the evaporation from the lake water surface and ΔV is the fluctuation in the volume of the lake water.

For the estimation of the inflows from the catchments, the Soil and Water Assessment Tool (SWAT) model [18,19] was applied. The input data required for the SWAT model are meteorological data (precipitation, temperature, relative humidity, wind speed and solar radiation) in the basin and the spatial information (elevation, land use, soil distribution) that compose the basin. The daily meteorological data (air temperature, dew point, air pressure, visibility, wind speed, precipitation) observed at Sidi Ahmed Air Base (Figure 1) were downloaded from the National Center for Environmental Information [20]. The catchments shown in Figure 1 were delineated based on ALOS-DSM [21]. Figure 4 shows the land use distribution map from the database of the European Space Agency [22] and the soil distribution map from the database of the Food and Agriculture Organization of the United Nations [23].
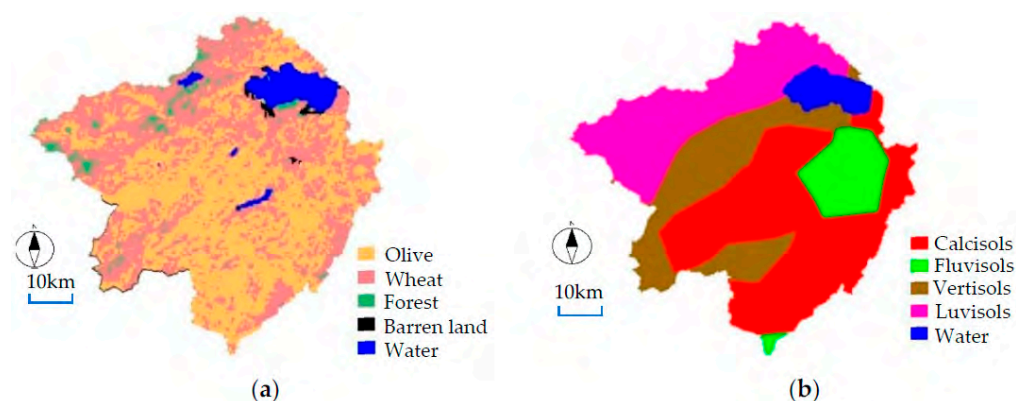
Figure 4. (**a**) Land use distribution and (**b**) Soil map of the catchments.

The inflows to each reservoir, estimated from the budget with the recorded intake, spillway, evaporation and water level (volume fluctuation) were used for calibration of the runoff model parameters with SWAT-CUP [24], the software optimizing the parameters using comparison with an observed discharge. According to the records of the management works of these reservoirs, almost all of the annual inflows were exploited (intake), except when the water level reaches the surcharge water level and there is an overflowing through the spillway. In addition, the inflows to Ichkeul Lake consist of not only the discharge from the reservoirs. There are some blanches that do not flow through the reservoirs. The applicability of the calibrated parameters to these residual catchments should be evaluated. So, the reliability of the parameters was confirmed as follows:

First, the parameters were calibrated with the inflow to Joumine reservoir. Then the parameters were applied to the catchment of Sejnane reservoir and the calculated discharge showed good agreement with the inflow to Sejnane reservoir. Table 1 shows the ranges of parameters used for the calibration with SWAT-CUP and the calibrated values. The range of parameters for the calibration refers to Mtibaa et al. [25] who studied the upstream area of the Joumine reservoir.

Table 1. Value ranges and calibrated values identified by SWAT-CUP for the Joumine reservoir catchment.

Parameter	Definition	Value Range	Calibrated Value
CNII.mgt	Runoff curve number for moisture condition II	±1	−0.405
ALPHA_BF.gw	Baseflow recession constant	0–1	0.968
GW_DELAY.gw	Groundwater delay	0–50	0.833
GWQMN.gw	Threshold water level in shallow aquifer for baseflow	0–500	82.5
CH_N1.rte	Manning's roughness coefficient for tributary channel	0–0.3	0.142
CH_K1.rte	Effective hydraulic conductivity in tributary channel alluvium (mm/h)	0–120	100.5
CH_N2.rte	Manning's roughness coefficient for main channel	0–0.3	0.221
CH_K2.rte	Effective hydraulic conductivity in main channel alluvium (mm/h)	0–120	19.78
SLSUBBSN.hru	Average slope length (m/m)	±0.2	−0.068
ESCO.hru	Soil evaporation compensation factor	0–1	0.168
REVAPMN.gw	Threshold water level in shallow aquifer for "revap"	0–100	60.83
RCHRG_DP.gw	Aquifer percolation coefficient	0–1	0.872
GW_REVAP.gw	Groundwater "revap" coefficient	0–1	0.685
Sol_AWC.sol	Soil available water content	±1	0.435
SOL_K.sol	Saturated hydraulic conductivity (mm/h):	±1	0.865
EPCO.hru	Plan evaporation compensation factor	0–1	0.402

Then those parameters were also applied to the residual catchments. The lake water level was calculated with all these simulated discharges from each catchment and the outflow from Tinja Channel mentioned later. However, the calculated water level did not show good agreement with the observed one. The cause of the error of the inflow is that the parameters determined in the Joumine basin were applied to the vast residual basin where the topography and geology are different from the catchment areas of both reservoirs. There is no record of discharge for calibrating the model parameters of the

residual catchment. Instead, the parameters were determined based on the runoff analysis of another catchment which is similar in topography and geology to the residual catchment. The catchment area of Masri dam is in the foothills of the Atlas Mountains with Calcisol the same as the residual catchment, but it is not in the Ichkeul basin. The runoff parameters were identified based on the time series of the discharge in the management record of this dam, and the same parameters were given to the residual basin of Ichkeul.

Data on pan evaporation could be obtained only from 2008 to 2010. Since the fluctuations of the values between years are small, average values of the 3 years on each date were used for the other years.

The outflow from the lake through Tinja channel was calculated using the Manning equation:

$$v = \frac{1}{n} R^{\frac{2}{3}} I^{\frac{1}{2}} \tag{2}$$

where v is the flow velocity (m/s), n is the Manning roughness coefficient (s/m$^{1/3}$), R is the hydraulic radius (m) and I is the gradient. The channel length and width required for this calculation are 4700 m and 33.7 m, respectively. Hydraulic radius was calculated based on the depth survey in the cross section shown in Figure 5. The roughness coefficient was given as 0.024.
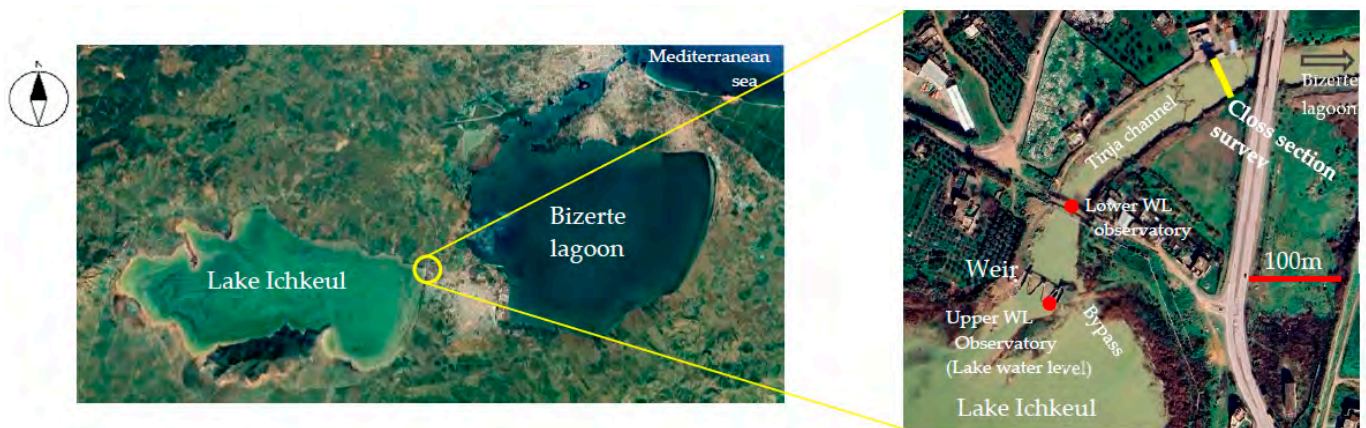
Figure 5. Location of the water level observatories on Tinja channel.

There is a tide stop weir at the entrance from the lake to the Tindja canal. The weir is closed when the lake water level is lower than the water level of the lagoon. However, besides the weir, there is the bypass on the right bank, allowing a little reverse flow in summer. Just after the construction of the weir, without the bypass, the tide was stopped completely in summer, but the evaporation was extreme and the salinity around the weir became higher than the seawater. Then the bypass was opened for dilution. So that, even when the weir is closed, there is a little reverse flow in summer.

The water levels upstream and downstream of the weir were observed only in 2015. The flow rate was calculated using the gradient from the water level on the downstream side of the weir to the average sea level of Bizerte lagoon. Then, the relationship between the water level of the upstream side of the weir (lake water level) and the flow rate estimated with the hydraulic gradient was found as shown in Figure 6. The relationship is for the term of the forward flow when the lake water level is high. In the same way, we also obtained a relationship with the lake water level for the reverse flow that occurs during the low water level period (Figure 7). High coefficient of determinations of 0.83 and 0.85 respectively, were found. When the lake water level falls below the average tide level of 0.53 m in Bizerte Lagoon, the tide stop weir might be closed for the regurgitation of seawater intrusion. As seen in the later figure showing the fluctuation of observed flow rate, the flow rate was 0 m^3/s when the water level was near 0.53 m.
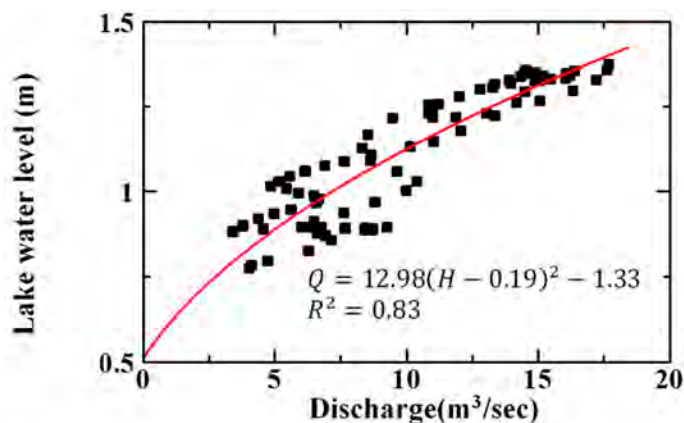
Figure 6. The relationship between the lake water level and the forward flow calculated from the gradient between the lower WL observatory and seawater level.
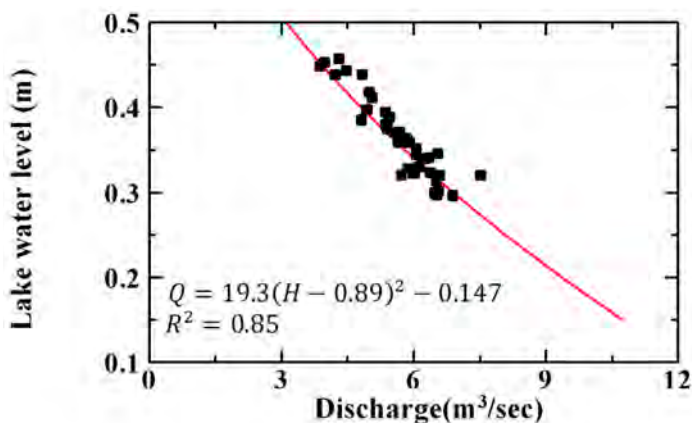

Figure 7. The relationship between the lake water level and the reverse flow from the lagoon to the lake calculated from the gradient between the lower WL observatory and seawater level.

Regarding the verification of this calculated outflow, there was no record observed in the field. The validity of the results was evaluated by the reproducibility of the lake water level obtained at the end of this water budget estimation.

The volume fluctuation of the lake on the right side of Equation (1) was converted into the fluctuation of the water level based on the relationship between the water level and the volume of water of the lake (Figure 8) obtained from the bathymetry map shown in Figure 3. Finally, the daily water level of the lake was calculated and evaluated with the observed data from 2002 to 2007.
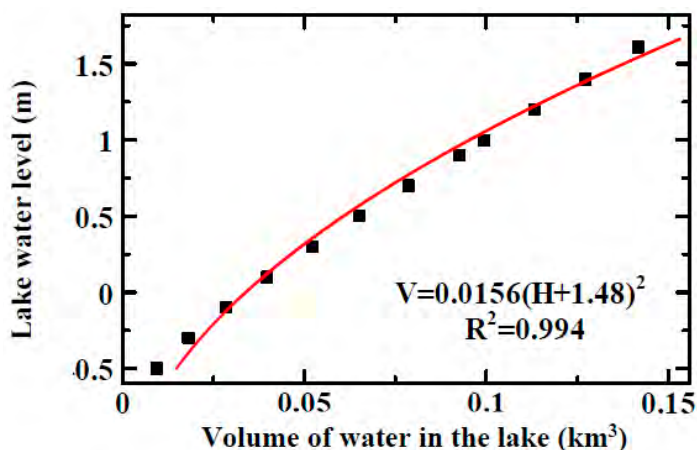

Figure 8. The relationship between volume and water level.

2.3. Modeling the Sediment Resuspension Driven by Wind

2.3.1. Related Studies on Resuspension

This study consists of three parts: runoff analysis from the upstream region, modeling of resuspension in the lake and the assessment of outflowing from the lake based on hydraulic estimation in Tinja canal. There are several approaches to the second part while the methods for the first and third parts are standard. Here, we will overview the conventional approaches regarding resuspension modeling. Bed erosion due to resuspension also affects the water flows that define the ecosystem and material transportation. So far, research has been conducted on various lakes [26–28], estuaries [29] and relatively shallow waters along the coast [30].

The driving force of resuspension is bed shear stress induced by the orbital velocity of waves, tidal current, storm surge and wind. In places where orbital velocity and current exist, such as estuaries and coastal areas, the shear stresses from both are considered linearly or nonlinearly. Previously, they were obtained as empirical formulas based on laboratory experiments [31–33]. Soulsby and Clarke [34] proposed a theoretical but practical formula for estimating total shear stress. On the other hand, shear stress in lakes is often estimated only by the orbital velocity because the current velocity is smaller in the lake than the orbital velocity [35]. First, the wave height was estimated from the wind stress, then it was converted to orbital based on the linear small-amplitude wave theory.

Wiberg and Sherwood [36] proposed a method to calculate the bed orbital velocity from the power spectrum of the flow velocity, but there are few studies in which the orbital velocity was observed. In the case of lakes, taking only wind waves into account, the bed shear stress was often estimated depending on whether the flow regime is laminar or turbulent [37]. Especially in an extremely shallow lake, the flow regime tends to be turbulent when strong winds continue, due to the passage of low pressure, monsoons and westerlies. However, few studies observed such typical events due to the difficulty of field observation under severe conditions. Lodahl et al. [38] showed that the critical Reynolds number was smaller when the oscillating flow and the unidirectional flow coexist in the pipeline than when only the oscillating flow exists. This fact suggests that the flow regime and bed shear stress change depending on whether there is only oscillating flow or the coexistence of oscillating and unidirectional flow.

The temporal fluctuation of the turbidity in a shallow lake was described with a box model that considers only the resuspension and the deposition of the fine sediment particles. The amount of sediment entrainment was expressed as a function of the bed shear stress. However, the parameters in the function were defined empirically. Hofmann [39] applied the model of the entrainment in a channel proposed by Garcia and Parker [40] to the lakebed resuspension in the shallow lake.

On the other hand, direct measurements of the velocity fluctuation in situ could be found. They were taken in a coastal shallow area using Acoustic Doppler Velocimetry (ADV) which measures three-dimensional instantaneous velocity with a high temporal frequency [41]. Hofmann et al. [39] carried out field observations at the lake with ADV. The results show a high contribution rate of orbital flow to the bed shear stress.

Sediment exchange and transportation between closed water bodies and river channels are understood based on two-dimensional or three-dimensional flow observations, remote sensing and modeling in lakes. Hawley et al. [42] discussed the transport mechanisms of SS in Lake Michigan using numerical simulation. Matty et al. [43] investigated the transportation of SS in Lake Houston. The intensity of the circulation in the lake was periodically high enough to transport coarse silt in suspension. Especially in shallow lakes where sediment transportation affects the hydrological system and environment, some researchers are paying attention to SS transport. Most of them have focused on runoff-induced dynamic conditions. Gao et al. [44] evaluated the impact of climate change and human activities on the sediment exchange process between Changjiang River and Poyang Lake. Zhang et al. [45] observed the fluctuation of the bed level of the lake due to erosion based on satellite image analysis. Wang [46] combined field data, laboratory

experiments and numerical simulations to try to understand the variation of SS in Poyang Lake. However, there are few studies evaluating the volume of transported sediment from a shallow lake to a lower basin based on the modeling of resuspension of sediment and hydrological runoff.

In this study, we observe horizontal two-dimensional velocity with an electromagnetic current meter that is cheaper than ADV. The vertical velocity was not observed but it was sufficient for the estimation of the Reynolds number and the bed shear stress in the shallow lake. The correlation between wind speed and Reynolds number was defined empirically using the observed data while that between Reynolds number and turbidity was found by laboratory experiment. The sediment outflow from Ichkeul Lake through the connecting channel was evaluated using the water exchange in the budget and the estimated turbidity. In this study, all kinds of data for the whole term were not available, but the field measurements, hydrological modeling and laboratory experiments complement each other and a long-term evaluation was carried out.

2.3.2. Box Model

Luettich et al. [47] showed the application of a simple box model for the resuspension of sediment driven by wind in a shallow lake. Assuming well mixing and negligible horizontal advection, the temporal fluctuation of the averaged concentration of suspended solids (hereinafter referred to as SS) in the column is expressed by the following equation:

$$h\frac{d\bar{c}}{dt} = w_s(E_s - \bar{c}) \tag{3}$$

where, h is the water depth of the column, w_s is the sedimentation speed of suspended particles (m/s) and E_s (kg/m^3) is the resuspension rate. Assuming that the disturbance caused by the wind is maintained for a certain period, the sedimentation and resuspension would be in equilibrium. In that case, the left side of the above equation can be zero.

On the other hand, resuspension occurs only when the bottom shear stress exceeds the critical tractive stress acts. That is expressed as the following formula:

$$E = w_s E_s = M(\tau - \tau_{cr})^n \tag{4}$$

where M and n are constants, τ is bottom shear stress and τ_{cr} is the critical bottom shear stress at which resuspension starts. n is given as 1 in some previous studies [48,49].

On the other hand, the bottom shear stress τ is modeled as a resuspension by the oscillating flow, it is expressed by the following equation:

$$\tau_w = \frac{1}{2}\rho_w f_w U_{bw}{}^2 \tag{5}$$

where, ρ_w (kg/m^3) is the density of water, f_w is friction coefficient and U_{bw} is the root mean square of the flow velocity (m/s). The bottom shear stress characteristics vary depending on the bottom roughness and flow conditions (turbulence/laminar flow) indicated with the Reynolds number defined by the kinematic viscosity coefficient ν(m^2/s) and predominant period T (s) as follows:

$$Re_w = \frac{U_{bw}{}^2 T}{2\pi\nu} \tag{6}$$

In case of laminar flow ($Re_w < 150{,}000$) that occurs through all terms in this study, f_w in (5) can be given as $2Re_w{}^{-0.5}$ [50]. Through Equations (3)–(6), the concentration of SS in an equilibrium state in which a constant disturbance continues can be expressed as a function of the Reynolds number. In this study, the relationship between the two will be formulated by laboratory experiments in Section 2.3.3, and then we tried to explain the results of field observations of flow velocities and turbidity, obtained in the center of the lake for a short period in the same manner, as shown in Section 2.3.4.

2.3.3. Laboratory Experiments

Laboratory experiments were carried out for formulating the relationship between the above mentioned Reynolds number and the concentration of SS using a vertical tank and stirring device as shown in Figure 9. The sediment sampled from Ichkeul Lake was used. Four stirrers were placed over the vertical tank (25 × 25 cm with 1 m depth). The fins of stirrers were placed near the water surface. The sensor of the velocity meter (KENEK, VMT2-200-04P) measuring horizontal 2D velocities was placed in the center at 40 cm depth from the water surface, 50 cm above the sediment surface. The sensor of the turbidity meter (KENEK, PM-501N) was also placed at the same depth but besides the center. Both the velocity and turbidity were measured at a frequency of 10 Hz.
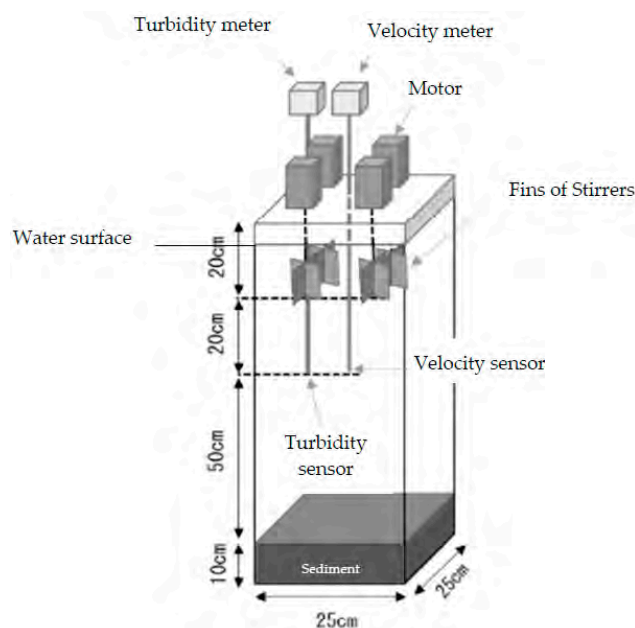
Figure 9. Experimental setup of sediment resuspension.

U_{bw} (cm/s) as the flow velocity amplitude and T as the predominant period of the fluctuating velocity were calculated from the continuous measured values under a steady equilibrium state with a constant rotation speed of the stirrer. The relationship between turbidity and SS (mg/L) is calibrated in advance, and the turbidity measurement value is converted to SS.

The experiments were conducted in summer and winter when the water temperatures were different, and the water temperature in summer was around 28 °C, while the water temperature in winter was around 10 °C. In addition, the tank prepared at the beginning of this study gave a uniform predominant period T that might depend on the size of the water tank. Therefore, the same experiment was conducted using other water tanks of different sizes, 40 × 40 cm and 1 m in height.

2.3.4. Field Observation

Flow velocity and turbidity at the center of the lake were observed continuously for one week in September 2015 and March 2016. A horizontal 2D electromagnetic current meter (Infinity-EM, JFE Advantech Co., Ltd., Kobe, Japan) and a turbidity meter (Infinity-CLW, JFE Advantech Co., Ltd.) were installed at a depth of 50 cm from the bottom of the lake, the same as the laboratory experiment mentioned above. A place without aquatic plants was selected for the installation. The recording was performed at 10 Hz for 30 s (300 samples) at 2 min intervals.

Wind speeds were observed at 1-h intervals from March 2015 to March 2016 near the entrance of the Tindja canal.

3. Results and Discussion

3.1. Estimation of Water Budget

3.1.1. Inflow from the Catchment Area

The calculated discharge from the catchment of Joumine reservoir, calibrated with SWAT-CUP has a good agreement with the observed discharge from September 2008 to September 2010 as shown in Figure 10. The discharge from the neighboring catchment, Sejnane reservoir, could be reproduced with the same parameter values as Joumine reservoir catchment, shown in Figure 11. Since the winter season is the rainy season and the summer season is the dry season in this study site, the figures start from September of each year, the beginning of the rainy seasons. Both agreements were quantitatively evaluated with the coefficients of determination, RMSE and NSE in Table 2. Comparing the observed and calculated values in Figures 8 and 9, the peak flow rate and the recession phase could be reproduced well. The coefficient of determination of the Joumine basin for 2009 is rather low, but 2009 was a dry year and the flow rate was small throughout the year.
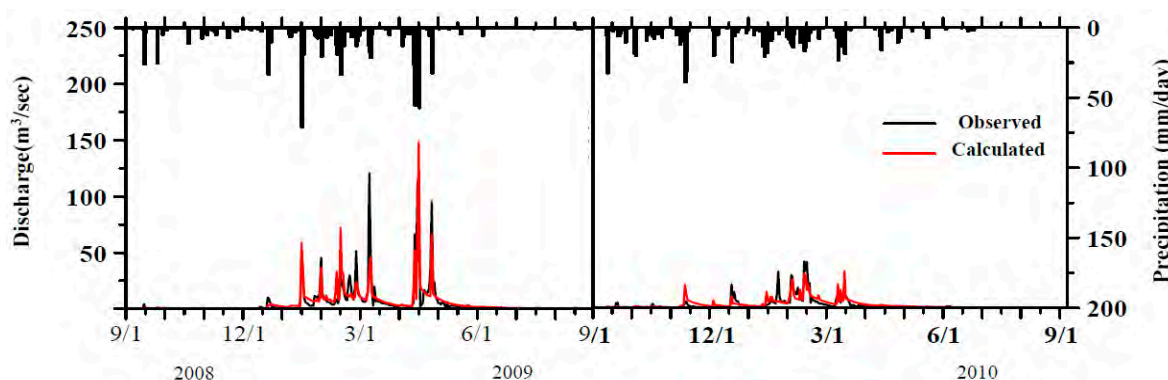

Figure 10. Simulation result of the discharge from Joumine reservoir catchment calibrated with SWAT-CUP.
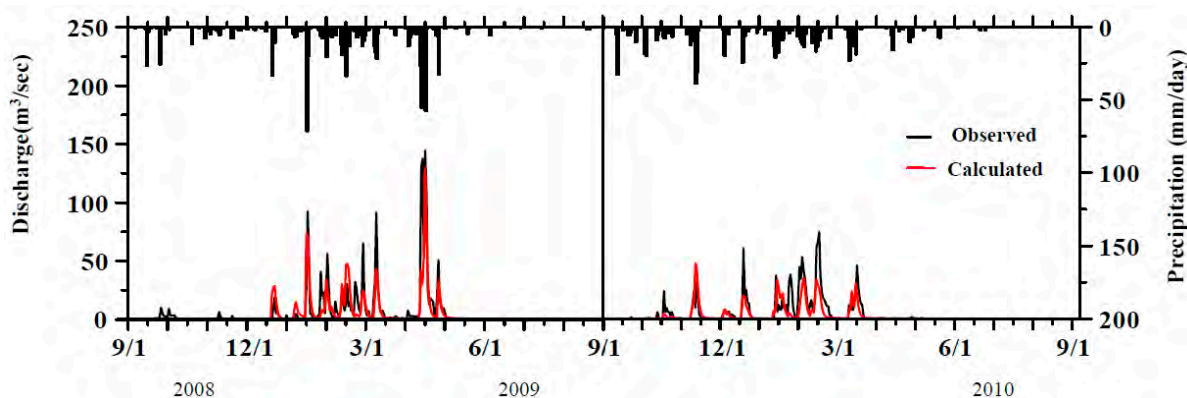

Figure 11. Simulation result of the discharge from Sejnane reservoir catchment with the parameters calibrated with Joumine reservoir catchment.

Table 2. Evaluation of the runoff simulations for the catchments of Joumine and Sejnane.

Catchment	Years (Precipitation)	R^2	RMSE	NSE
Joumine	2008 (836 mm)	0.7	7.57	0.68
	2009 (757 mm)	0.58	3.46	0.18
	2008–2009	0.68	5.01	0.63
Sejnane	2008 (836 mm)	0.64	10.73	0.70
	2009 (757 mm)	0.52	7.42	0.54
	2008–2009	0.62	7.90	0.65

Based on these results, the mountainous catchments upstream of the two reservoirs have similar morphology and hydrological characteristics, so both discharges could be explained with the same parameters. On the other hand, the residual catchments without the records of the discharges have different characteristics. As mentioned in Section 2.2, the parameters calibrated for the hilly catchment with Calcisol soil were given to the lower hilly area of the study site. Finally, the acceptable calculation results of the lake water level were obtained as shown in the later chapter.

3.1.2. Fluctuation of Water Level and Volume

The change in the water in the lake was calculated from the inflow and outflow obtained using the above procedure. The evaporation from the lake surface was considered the same as the record of the pan evaporation at Joumine dam office. From the net water volume change in the lake, the water level of the next day was sequentially calculated for the rainy season in 2015 when we installed the water level gauges in Tinja channel. The time series of the calculated outflow from the lake changes more slowly than the inflow due to the storage effect of the lake (Figure 12). The lake water level reproduced from these calculated discharges and the bathymetry of the lake were compared with the observed lake water level in 2015 as shown in Figure 13. The calculation period started when the lake level exceeded the average sea level and the forward outflow from the lake to the lagoon occurred on 28 January. The error between the calculated and observed water level in the second half shown in Figure 13 reached more than 10 cm but the tendency is similar. The coefficient of determination with the measured water level was 0.89 and the RMSE was 0.092. Since 2015 was a drought year, it is probable that the accuracy of the inflow was particularly low as mentioned in Section 3.1.1 and that errors were likely to be comparatively large.
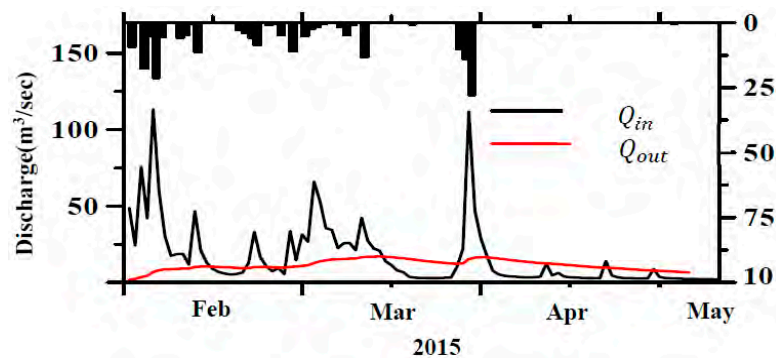

Figure 12. The simulated total inflow to, and outflow from, the lake (2015: rainy season).
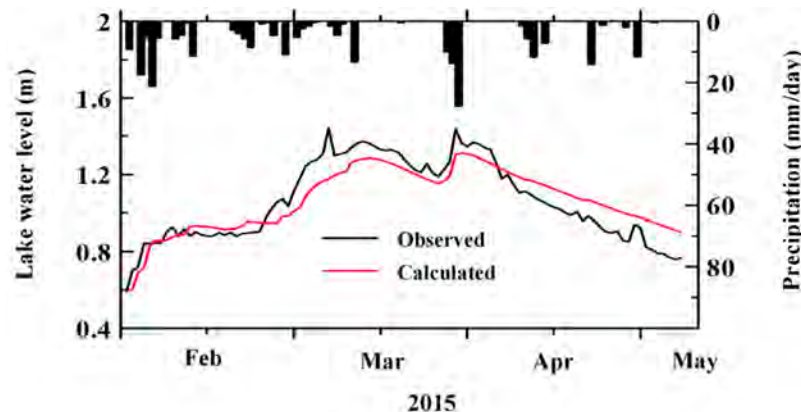

Figure 13. The simulated lake water level: the SWAT parameters calibrated with Masri reservoir catchment (Hilly and Calcisol soil) were applied to the lower catchment. The parameters used for the mountainous catchment were calibrated with Joumine reservoir catchment.

The identified parameters were applied to the longer simulation and verified with the water level record. The results of the lake water level calculated only from precipitation and evaporation over a long term were compared with the water level observed by the National Agency of Protection of the Environment (ANPE) [51] in Figure 14. The reproducibility of the water level fluctuation in the high rainfall year is high, and the water level fluctuation could be re-produced even over a long period.
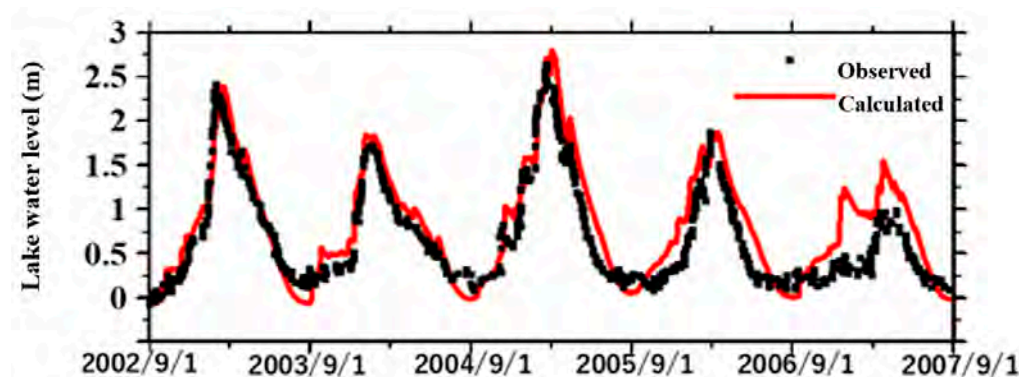

Figure 14. The simulated lake water level verified with the long term observed data.

3.1.3. Water Budget of the Lake and Influence of the Reservoirs

Based on the water budget model mentioned above, the annual water budget from 2000 to 2018 was calculated. Water intakes and discharge downstream at the reservoirs in Table 3 were the recorded data in the dam management reports. As mentioned, here the same values as the average of 2008–2010 pan evaporation at Joumine reservoirs were given for each year.

Table 3. Annual water budgets from September 2000 to August 2019 under the current state.

							(Unit: Million m^3)
				Current State			
	Reservoirs				Ichkeul Lake		
Years (September–August)	Intake (Exploitation)	Evaporation	Disch. to Downstream	Total Inflow	Precipitation	Evaporation	Outflow	Reverse Flow
2000–2001	52	56	0	99	39	249	29	140
2001–2002	82	56	0	72	36	309	3	204
2002–2003	92	56	292	486	58	309	351	115
2003–2004	109	56	112	393	71	309	227	72
2004–2005	88	56	268	733	82	309	571	65
2005–2006	165	56	112	405	49	309	248	103
2006–2007	152	56	2	290	59	309	152	111
2007–2008	174	56	3	308	57	309	163	106
2008–2009	158	56	91	453	74	309	303	86
2009–2010	167	56	57	336	67	309	205	111
2010–2011	186	56	1	206	54	309	91	140
2011–2012	193	56	254	600	77	309	476	109
2012–2013	180	56	58	283	65	309	162	123
2013–2014	187	56	48	288	61	309	155	116
2014–2015	199	56	35	247	59	309	136	139
2015–2016	152	56	0	125	42	309	26	168
2016–2017	127	56	0	215	56	309	122	161
2017–2018	141	56	0	186	69	309	64	117
2018–2019	165	56	66	324	63	309	179	101

In order to compare the water and sediment budgets between the states with and without the reservoirs, the water budgets with the reservoirs were also simulated. The fluctuation of the simulated lake water level, assuming no upstream reservoirs, is shown as the red line in Figure 15. Due to the water storage effect of the reservoirs, the inflow was reduced and the rise in the lake level was suppressed. Especially in drought or moderate years, when there is almost no spilling from the dam, the difference in the peak of the lake water level is large. The water budget by year.
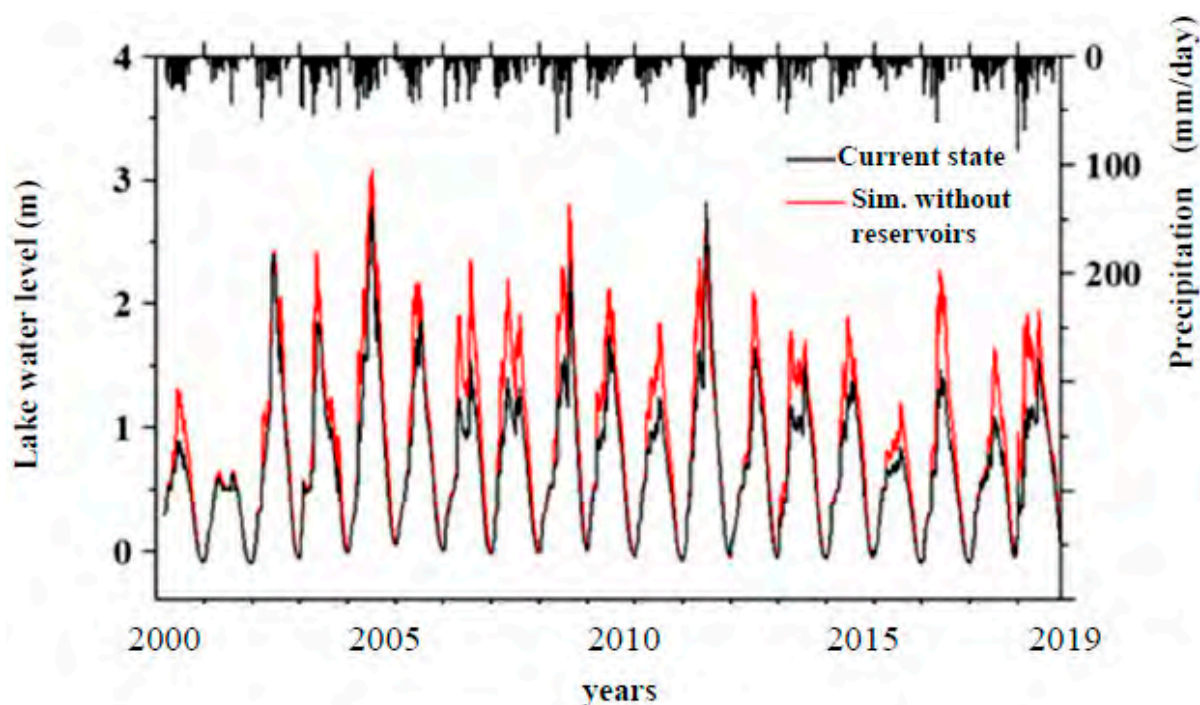
Figure 15. The simulations of the water level of the lake for 19 years (September 2000–2019).

The effect of the tide stop weir could be confirmed from the ratio of the current state and the simulation without the reservoirs as shown in Table 4. The total inflow and outflow were drastically reduced by the reservoirs, but the increase in the reverse flow of seawater was suppressed to within about 20%. The total inflows and outflows estimated with the water budget model were compared between the current state and the case without reservoirs. The results during the winter, from 1 September 2003 to 1 September 2006, are shown in Figure 16 as examples. In the case of "without reservoirs", larger peak discharges were found, and the outflow increased slightly due to the rise of the lake water level.

Table 4. Annual water budgets of the simulation without the reservoirs.

|				Outflow		Reverse Flow		(Unit: Million m^3)
Years (September–August)	Total Inflow	Precipitation	Evaporation	Current State	/without Dams (%)	Current State	/without Dams (%)	
2000–2001	171	39	249	88	33	127	110	
2001–2002	81	36	309	7	46	199	103	
2002–2003	408	58	309	434	81	277	42	
2003–2004	551	71	309	365	62	52	138	
2004–2005	986	82	309	823	69	64	101	
2005–2006	537	49	309	379	65	102	101	
2006–2007	561	59	309	397	38	86	129	
2007–2008	617	57	309	442	37	77	138	
2008–2009	732	74	309	563	54	67	128	
2009–2010	514	67	309	367	56	95	117	
2010–2011	373	54	309	242	38	125	113	
2011–2012	695	77	309	568	84	105	103	
2012–2013	399	65	309	265	61	110	111	
2013–2014	460	61	309	303	51	91	127	
2014–2015	391	59	309	265	51	124	112	
2015–2016	191	42	309	76	34	152	111	
2016–2017	445	56	309	335	36	144	112	
2017–2018	330	69	309	200	32	110	106	
2018–2019	514	63	309	331	54	63	160	
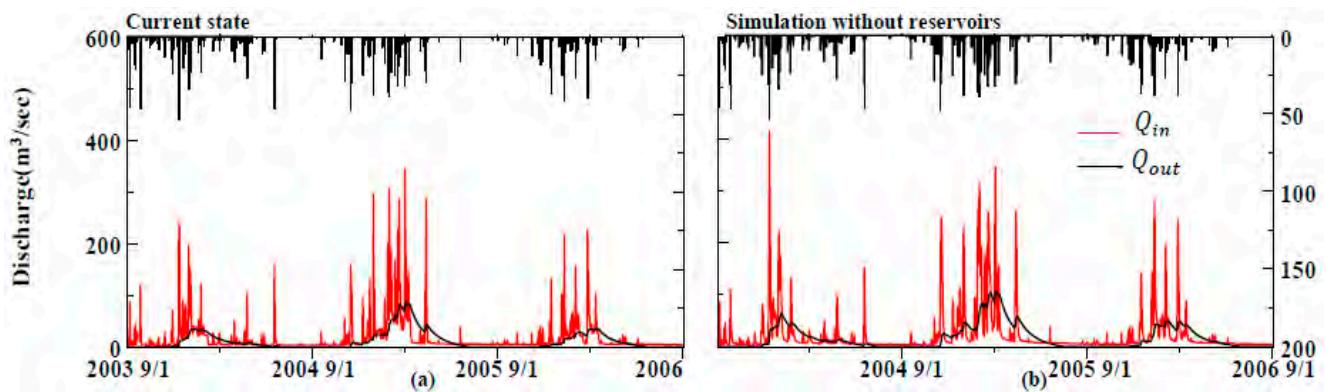
Figure 16. The simulations of the total inflow to, and outflow from, the lake: (**a**) the simulation of the current state (**b**) the simulation without the reservoirs.

3.2. Modeling of Resuspension Driven by Wind

3.2.1. Results of Laboratory Experiments and Field Observation

In the laboratory experiment, the rotation speed of the stirrer was kept constant so that the resuspension and settlement were in equilibrium and the turbidity approached asymptotically to a constant value. In the example of the record of SS and flow velocity shown in Figure 17, the rotation speed of the stirrer is increased in four steps. The SS increases as the flow velocity increases. The period during which the measured SS was stable at each stage was analyzed. The predominant period T was obtained by Fourier analysis of the fluctuation of the absolute flow velocity from the flow velocity in two horizontal directions measured by the current meter, and the root mean square U_{bw} of the flow velocity was obtained.
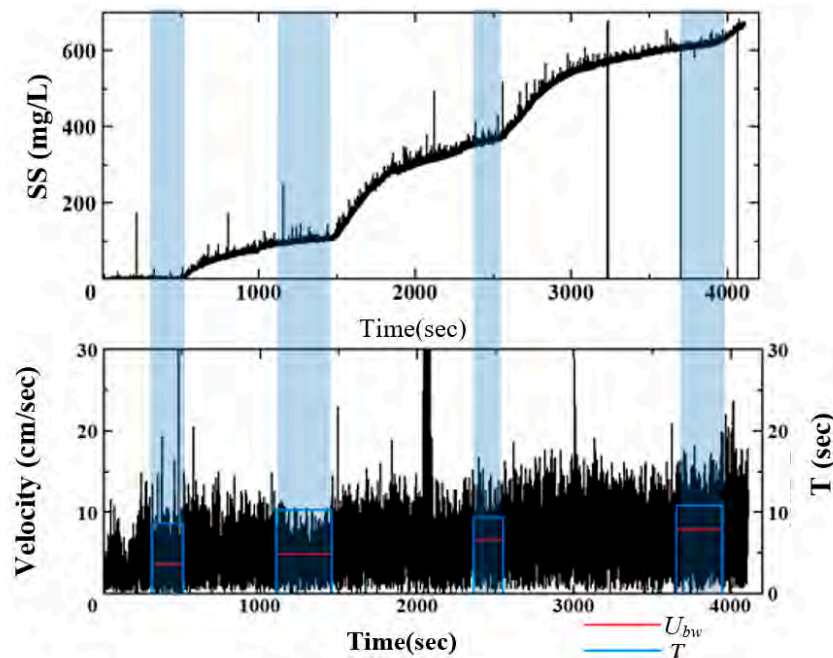
Figure 17. Example of results of the laboratory experiments. T as the blue bars were obtained from the fluctuation of the velocity with Fourier analysis.

It was expected that the turbulence intensity (Re_w) and SS would correlate, but the relationship would change depending on some factors because the state of the sediment surface seemed to change depending on the water temperature. First, when all the experimental results are shown in the same plot in Figure 18, the effect of water temperature that was initially expected was not large, and SS and turbulence intensity were in a linear relationship.
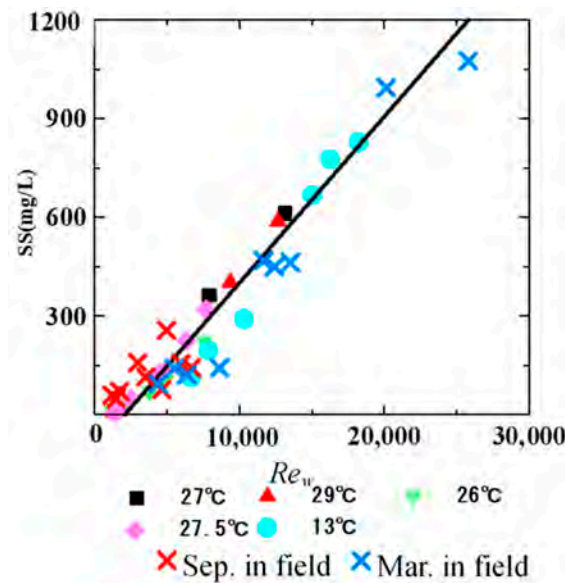
Figure 18. The relationship between turbulent intensity (Re_w) and the concentration of suspended solids.

The relationship between Re_w and SS observed in the field was also investigated. The hourly average of T, U_{bw} and Reynolds number were estimated from the time series of velocity observed in the field in September 2015 and March 2016 as shown in Figure 19. The period in which SS was stable for about an hour was extracted, and the relationships with the turbulence intensity and wind speed in the meantime were evaluated. The turbulence increased more in March when the westerlies occurred than in September, and the sediment was highly resuspended. No significant fluctuations were observed in the predominant period T in the field observation results, suggesting that the increase in the Reynolds number is highly dependent on U_{bw}.
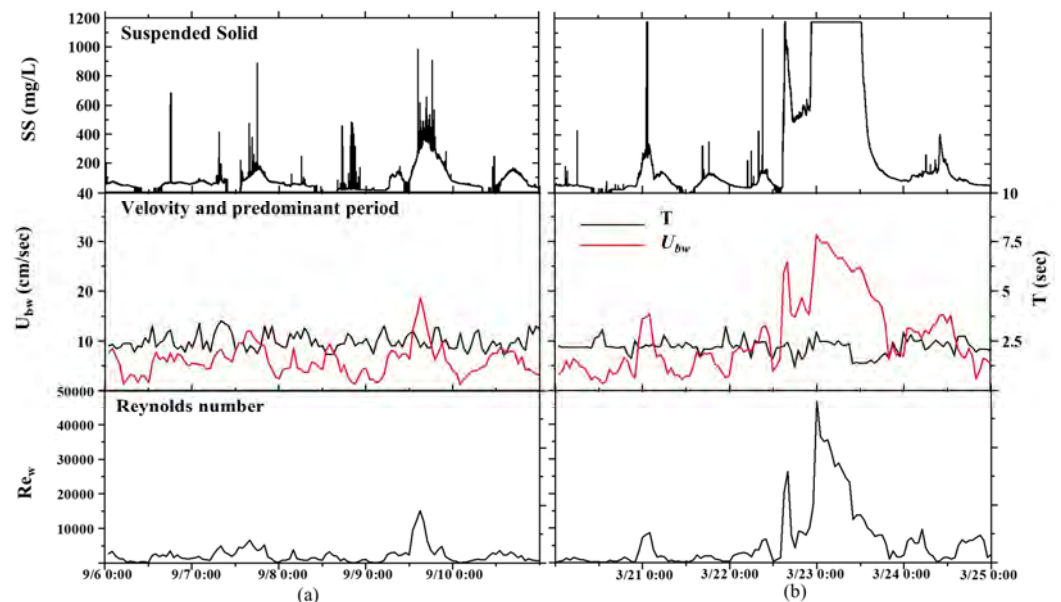

Figure 19. Results of the field observations: (**a**) September 2015 (**b**) March 2016.

The relationships between the Reynolds number and SS obtained from the results of field observations were shown as x marks in Figure 18. Those were on the same linear line as the results of the laboratory experiment. It is considered that the formulation of the relationship between the Reynolds number and SS in the laboratory experiment can reproduce the state of resuspension driven by wind in the field.

3.2.2. Relationship between Wind and Reynolds Number

The relationship between the wind speed observed in the field and the Reynolds number indicating the turbulence intensity hourly observed in the field is shown as the red rectangle in Figure 20. As the wind speed increased, the turbulence intensity increased exponentially. The coefficient of determination for the relationship was 0.90. However, the hourly wind data were not observed in the long term, while the daily average wind speed was available from the NOAA [51] database. Therefore, the relationship between the daily average of the Reynolds numbers and wind speed was obtained from the above hourly observed data. It is shown as the blue triangles in Figure 20. Even the daily averaged Reynolds number and wind speed showed the same relationship.
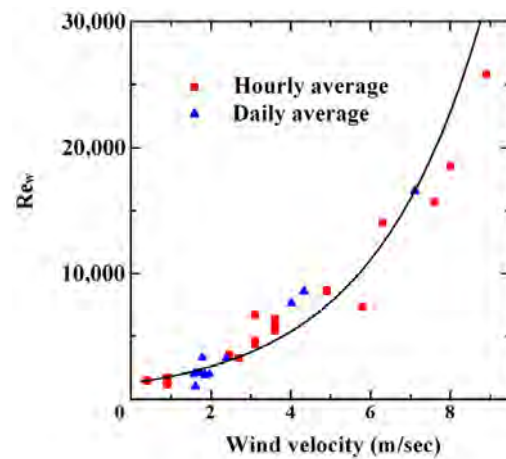

Figure 20. The relationship between the wind velocity and Reynolds number observed in the field.

Another concern is the location of the observatories. Sidi Ahmed Air Base, the observatory of NOAA, is located in Bizerte city which has a different wind speed from the lake. The wind speed downloaded from NOAA and the average daily wind speed observed near the lake for the two weeks when the hourly data were obtained were not equal but were highly correlated, with a coefficient of determination of 0.946 as shown in Figure 21. The temporal fluctuation of the Reynolds number was estimated from the daily wind speed data downloaded from NOAA through the two relationships identified in Figures 20 and 21. The time series of SS estimated from the NOAA wind velocity data was verified by the comparison with the daily average SS measured in the field from 6 September to 11 September and 20 March to 24 March (Figure 22) The daily averaged concentration of SS was well reproduced, especially in winter.
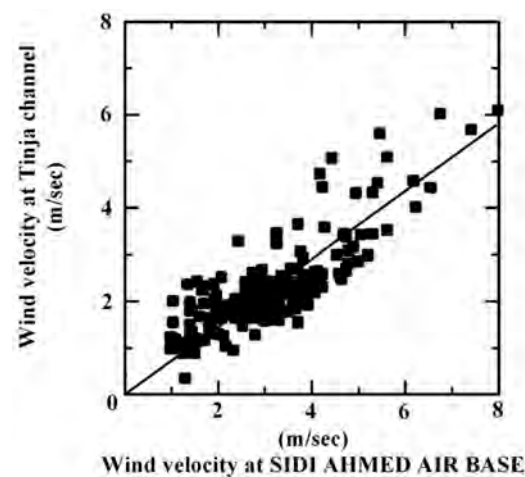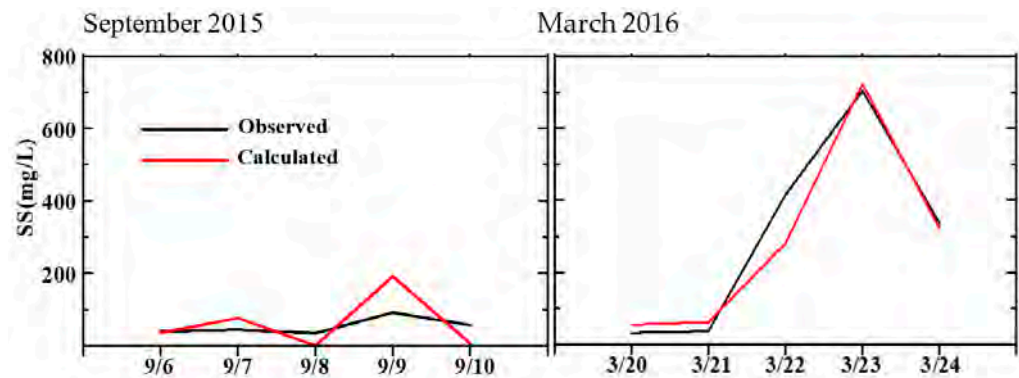

Figure 21. The comparison of wind velocities between Sidi Ahmed Air Base and Tinja channel for the observation periods.

Figure 22. The daily average of the concentration of SS in the lake in the observed periods estimated from wind velocity data.

3.2.3. Estimation of the Sediment Outflow

Using a combination of the water budget model and the wind resuspension model, the sediment transportation from the lake through Tinja channel was estimated for both cases: the current state and that without reservoirs, using the rainfall and wind speed data as input values. The time series of SS was estimated from the daily average wind speed. The change of SS due to the rise in the lake water level in the case without the reservoirs was not necessary to consider because it is assumed that the resuspension and settlement of the sediment were in an equilibrium state under constant wind speed for each day. Therfore, the same time series of SS shown in Figure 23 was used for both simulations with/without the reservoirs. Due to the increase in the water outflow to the lagoon, the sediment outflow in the simulation without the reservoirs was higher than the current state, as shown in Figure 24.
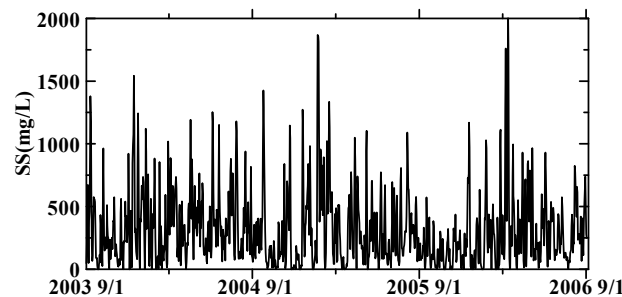
Figure 23. Turbidity in the lake estimated from the daily wind velocity at Sidi Ahmed Air Base.
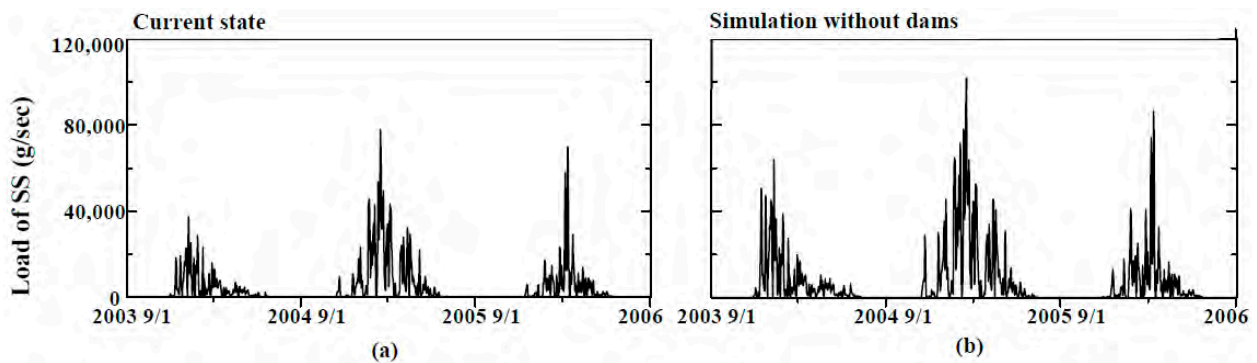
Figure 24. The flux of SS outflowing from the lake to the lagoon: (**a**) the simulation of the current state (**b**) the simulation without the dams.

The annual cumulative water discharge and the sediment transportation from the lake to the lagoon for each year were calculated (Figure 25). In drought years, the total amount of sediment outflow decreases as the amount of water discharge decreases. In this study,

the sediment yield in the upstream catchment was not estimated with SWAT because we could not obtain the observed data for calibration, but the SS concentration in the lake is considered to be independent of that of the inflow in such large and shallow lakes. It was modeled as being highly dependent on wind disturbance intensity. The available data representing the inflow of the solid matter to the lake is sedimentation in the reservoirs. Before the construction of the dams, the trapped sediment in the reservoirs was the supply of sediment to the lake.
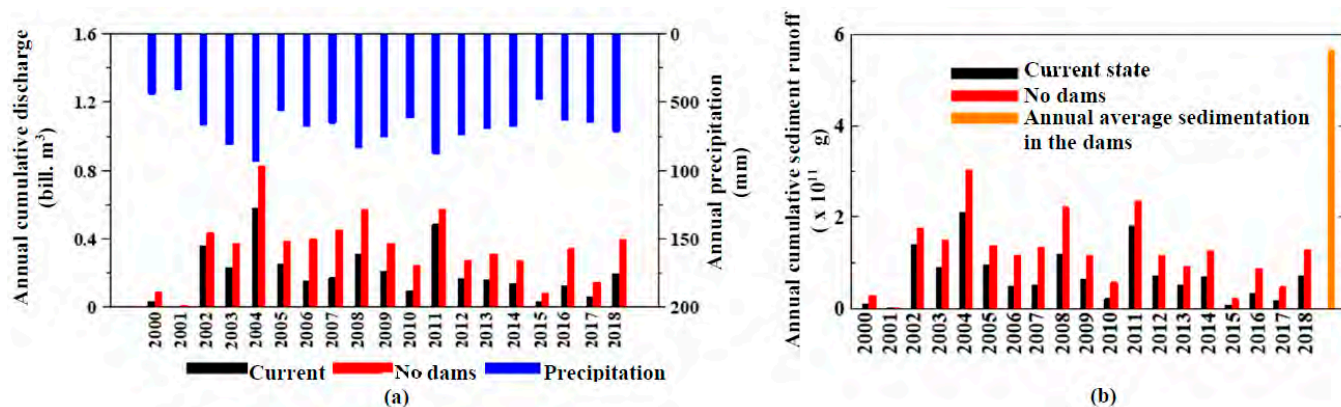
Figure 25. Comparison between the cases with/without dams: (**a**) Annual cumulative discharge and (**b**) Annual cumulative sediment runoff.

The orange bar in the right Figure is the annual average sediment accumulation in the reservoirs, calculated from the bathymetric survey [38]. As it was larger than the outflow of the sediment in both cases, the lake originally tended to deposit sediment. However, after the reservoirs were constructed, the sediment supply (equivalent to the orange bar) had been almost cut off due to the sedimentation in the reservoirs while the sediment outflow continues. As a result, the sediment balance of the lake is negative and the altitude of the lakebed was decreasing, enhancing the seawater intrusion from the lagoon during the summer season.

4. Conclusions

In this study, the water budget of the brackish lakes and the resuspension caused by wind disturbance were modeled for evaluation of the changes in the sediment outflow due to the construction of the reservoirs. The sediment outflow from the lake was estimated only with the meteorological data as input, which is relatively easy to obtain.

Regarding the modeling of the water budget, the inflows from the catchments were estimated using SWAT, and the outflow was estimated from the hydraulic gradient between the lake water and the seawater level. Finally, the fluctuation of the lake water level in the long term was reproduced.

The resuspension process in the lake was described with a simple box model with fixed lakebed altitude in this study. We formulated the relationships between the wind, turbulent intensit, and sediment resuspension on the lake, based on laboratory experiments and field measurements. A uniform relationship between the turbulence intensity and resuspension was found in both the results of the experiments and the field measurements, while the wind and the turbulence intensity were formulated based on the results of field observations. The concentration of the SS in the lake was estimated only from the wind speed data.

The sediment transportation outflowing from the lake was simulated using a combination of the above two modelings. Compared to the annual average sedimentation in the upstream reservoirs, Ichkeul Lake tended to deposit sediments before the reservoirs were constructed. However, after the construction of the dams, the inflow of sediment from the inflowing river was almost cut off, and it was estimated that the outflow of sediment

might be excessive. It was suggested that the lake water level decreased and the saltwater intrusion to Ichkeul Lake increased as the lakebed was eroded.

In this study, the inflows of the sediment from the upstream catchments were not simulated in the budget. Whether the sedimentation tendency is erosive or cumulative was discussed using comparison to the annual average sedimentation in the upstream reservoirs. An alternative would be to compare with a more accurate estimate of soil yield in the catchments using SWAT instead of the annual average sedimentation of the upstream reservoir. However, we could not obtain the sediment load observed in the field for the verification of the results calculated using SWAT. In addition, the change of the altitude of the lakebed due to erosion or sedimentation was not considered and its steady state as the same bathymetry as that observed in 2015 was assumed. If the sedimentation tendency continues, as in the absence of dams, salt intrusion will be more restricted. On the contrary, if the sedimentation of the dam continues as it is and the elevation of the lake bottom continues to decrease, the salinity of Ichkeul Lake will be even higher due to the significant reverse flow from Bizerte Lagoon.

Currently, the environmental conservation of Ichkeul Lake is planned only with the focus on its water budget and the regulation of the lake water level. However, the lakebed depression due to the imbalance of the sedimentation also has a certain negative environmental impact on Ichkeul Lake. In further studies, it is expected to allow SWAT or other river basin scale models to be calibrated based on field observations of wash load and to assess soil yield in the catchments more precisely. In addition, to consider specific measures against the sediment budget imbalance, such as relocation of the sediment in the reservoirs to the lake, it is necessary to develop a model that can reproduce the changes in lakebed altitude caused by resuspension and sedimentation processes and evaluate the changes in saltwater inflow more accurately. This study, which showed that the tendency of sediment movement changed to erosive after the construction of the reservoirs in the upstream area, was the initiation for a more detailed examination.

Author Contributions: Conceptualization, M.I. and J.T.; methodology, M.I.; validation, M.I. and H.K.; formal analysis, M.I. and A.K.; investigation, M.I., A.K. and H.O.; resources, M.I. and J.T.; data curation, M.I., H.K. and H.O.; writing—original draft preparation, M.I., H.K. and A.K.; writing—review and editing, M.I.; visualization, M.I. and H.K.; supervision, M.I., A.K. and J.T.; project administration, M.I.; funding acquisition, M.I. All authors have read and agreed to the published version of the manuscript.

Data Availability Statement: Not applicable.

References

1. Miller, R. Forcing uncertainty and salinity response to dredging in a tidal freshwater river. *Int. J. River Basin Manag.* **2021**, 1–9. [CrossRef]
2. Yuan, R.; Zhu, J. Saltwater Intrusion in the Pearl River Estuary. *J. Coast. Res.* **2015**, *316*, 1357–1362. [CrossRef]
3. van Dijk, W.M.; Cox, J.R.; Leuven, J.R.; Cleveringa, J.; Taal, M.; Hiatt, M.R.; Sonke, W.; Verbeek, K.; Speckmann, B.; Kleinhans, M.G. The vulnerability of tidal flats and multi-channel estuaries to dredging and disposal. *Anthr. Coasts* **2020**, *4*, 36–60. [CrossRef]
4. Dias, J.M.; Pereira, F.; Picado, A.; Lopes, C.L.; Pinheiro, J.P.; Lopes, S.M.; Pinho, P.G. A Comprehensive Estuarine Hydrodynamics-Salinity Study: Impact of Morphologic Changes on Ria de Aveiro (Atlantic Coast of Portugal). *J. Mar. Sci. Eng.* **2021**, *9*, 234. [CrossRef]
5. Anthony, E.; Brunier, G.; Besset, M. Linking rapid erosion of the Mekong River delta to human activities. *Sci. Rep.* **2015**, *5*, 14745. [CrossRef]
6. Kondolf, G.M.; Rubin, Z.K.; Minear, J.T. Dams on the Mekong: Cumulative sediment starvation. *Water Resour. Res.* **2014**, *50*, 5158–5169. [CrossRef]
7. Milliman, J.D.; Syvitski, J.P.M. Geomorphic/Tectonic Control of Sediment Discharge to the Ocean: The Importance of Small Mountainous Rivers. *J. Geol.* **1992**, *100*, 525–544. [CrossRef]

8. Lu, X.X.; Siew, R.Y. Water discharge and sediment flux changes over the past decades in the Lower Mekong River: Possible impacts of the Chinese dams. *Hydrol. Earth Syst. Sci.* **2006**, *10*, 181–195. [CrossRef]

9. Irie, M.; Kashiwagi, K.; Ujiie, K.; Nsiri, I.; Bouguerra, S.; Tarhouni, J. Feasibility of Exploitation of the Sediment in the Reservoirs for the Sustainability of Surface Water Resource in Tunisia. *J. Jpn. Soc. Civ. Eng. Ser. G* **2012**, *68*, II41–II46. [CrossRef]

10. Irie, M.; Kawachi, A.; Nsiri, I.; Tarhouni, J. Observation of floodwater behavior and sedimentation in the reservoir. *J. Jpn. Soc. Civ. Eng. Ser. B1* **2013**, *69*, 247–252.

11. Hata, T.; Irie, M.; Kawachi, A.; Tebakari, T. Evaluation of sediment solidification ability using in situ microbial functions in Ichkeul Lake, Tunisia. *Euro-Mediterr. J. Environ. Integr.* **2016**, *1*, 2. [CrossRef]

12. Barhoumi, B. Biomonitoring Pollution of the Bizerte Lagoon (Tunisia) by Comparative Analysis of Contamination Levels and Ecotoxicity of Sediments and Biota. Ph.D. Thesis, Université de Bordeaux, Bordeaux, France, 2014. (In French).

13. So, S.; Khare, Y.; Mehta, A. Critical wind and turbidity rise in a shallow Florida lake. *WIT Trans. Ecol. Environ.* **2013**, *169*, 13. [CrossRef]

14. Béjaoui, B.; Harzallah, A.; Moussa, M.; Chapelle, A.; Solidoro, C. Analysis of hydrobiological pattern in the Bizerte lagoon (Tunisia). *Estuar. Coast. Shelf Sci.* **2008**, *80*, 121–129. [CrossRef]

15. Ouni, H.; Kawachi, A.; Irie, M.; Ben'Barek, N.; Hariga-Tlatli, N.; Tarhouni, J. Development of water turbidity index (WTI) and seasonal characteristics of total suspended matter (TSM) spatial distribution in Ichkeul Lake, a shallow brackish wetland, Northern-East Tunisia. *Environ. Earth Sci.* **2019**, *78*, 228. [CrossRef]

16. Hata, T.; Irie, M. Evaluation of sediment solidification ability using in situ microbial functions in Ichkeul Lake, Tunisia. *J. Jpn. Soc. Civ. Eng. Ser. G* **2013**, *71*, 125–133. [CrossRef]

17. Irie, M.; Taga, S.; Tarhouni, J.; Fuji, M. Trial Production of Porous Ceramics Filter Made from Sediments in Water Reservoirs for Sustainable Use of Surface Water Resource in Arid Land. *Int. J. Environ. Sci. Dev.* **2017**, *8*, 549–556. [CrossRef]

18. Van Liew, M.W.; Garbrecht, J. Hydrologic Simulation of the Little Washita River Experimental Watershed Using SWAT. *J. Am. Water Resour. Assoc.* **2003**, *39*, 413–426. [CrossRef]

19. Briak, H.; Mrabet, R.; Moussadek, R.; Aboumaria, K. Use of a calibrated SWAT model to evaluate the effects of agricultural BMPs on sediments of the Kalaya river basin (North of Morocco). *Int. Soil Water Conserv. Res.* **2019**, *7*, 176–183. [CrossRef]

20. National Centers for Environmental Information (NOAA). Available online: https://www.ncei.noaa.gov/data/global-summary-of-the-day/access/ (accessed on 31 March 2022).

21. ALOS World 3D. Available online: https://www.eorc.jaxa.jp/ALOS/en/aw3d30/data/index.htm (accessed on 31 March 2022).

22. ESA CCI Land Cover 20 m Map of Africa. Available online: http://2016africalandcover20m.esrin.esa.int/download.php (accessed on 31 March 2022).

23. FAO Map Catalog. Available online: http://www.fao.org/geonetwork/srv/en/metadata.show?id=14116 (accessed on 31 March 2022).

24. SWAT-CUP. Available online: https://www.2w2e.com/home/SwatCup (accessed on 31 March 2022).

25. Mtibaa, S.; Hotta, N.; Irie, M. Analysis of the efficacy and cost-effectiveness of best management practices for controlling sediment yield: A case study of the Joumine watershed, Tunisia. *Sci. Total Environ.* **2018**, *616–617*, 1–16. [CrossRef]

26. de Vicente, I.; Cruz-Pizarro, L.; Rueda, F.J. Sediment resuspension in two adjacent shallow coastal lakes: Controlling factors and consequences on phosphate dynamics. *Aquat. Sci.* **2010**, *72*, 21–31. [CrossRef]

27. Wang, P.; Hu, B.; Wang, C.; Lei, Y. Phosphorus adsorption and sedimentation by suspended sediments from Zhushan Bay, Taihu Lake. *Environ. Sci. Pollut. Res.* **2015**, *22*, 6559–6569. [CrossRef] [PubMed]

28. Hamilton, D.P.; Mitchell, S.F. An empirical model for sediment resuspension in shallow lakes. *Hydrobiologia* **1996**, *317*, 209–220. [CrossRef]

29. Zhu, Q.; van Prooijen, B.; Wang, Z.B.; Ma, Y.X.; Yang, S.L. Bed shear stress estimation on an open tidal flat using in situ measurement. *Estuar. Coast. Shelf Sci.* **2016**, *182*, 190–201. [CrossRef]

30. Wright, L.D.; Boon, J.D.; Kim, S.C.; List, J.H. Modes of cross-shore sediment transport on the shoreface of the Middle Atlantic Bight. *Mar. Geol.* **1996**, *96*, 19–51. [CrossRef]

31. Grant, W.D.; Madsen, O.S. Combined wave and current interaction with a rough bottom. *J. Geophys. Res. Oceans* **1979**, *84*, 1797–1808. [CrossRef]

32. Garcia, M.; Parker, G. Experiments on the entrainment of sediment into suspension by a dense bottom current. *J. Geophys. Res.* **1993**, *98*, 4793–4807. [CrossRef]

33. Soulsby, R.L.; Hamm, L.; Klopman, G.; Myrhaug, D.; Simons, R.R.; Thomas, G.P. Wave-current interaction within and outside the bottom boundary layer. *Coast. Eng.* **1993**, *21*, 41–69. [CrossRef]

34. Soulsby, R.L.; Clarke, S. *Bed Shear-Stresses under Combined Waves and Currents on Smooth and Rough Beds*; Report TR 137; Defra project FD1905; Hydraulics Research: Wallingford, UK, 2005.

35. Zikhali, V.; Tirok, K.; Stretch, D. Sediment resuspension in a shallow lake with muddy substrates: St Lucia, South Africa. *Cont. Shelf Res.* **2015**, *108*, 112–120. [CrossRef]

36. Wiberg, P.L.; Sherwood, C.R. Calculating wave-generated bottom orbital velocities from surface-wave parameters. *Comput. Geosci.* **2008**, *34*, 1243–1262. [CrossRef]

37. Carlin, J.A.; Lee, G.-H.; Dellapenna, T.M.; Laverty, P. Sediment resuspension by wind, waves, and currents during meteorological frontal passages in a micro-tidal lagoon. *Estuar. Coast. Shelf Sci.* **2016**, *172*, 24–33. [CrossRef]

38. Lodahl, C.R.; Sumer, B.M.; Fredsøe, J. Turbulent combined oscillatory flow and current in a pipe. *J. Fluid Mech.* **1998**, *373*, 313–348. [CrossRef]

39. Hofmann, H.; Lorke, A.; Peeters, F. Wind and ship wave-induced resuspension in the littoral zone of a large lake. *Water Resour. Res.* **2011**, 47. [CrossRef]

40. Garcia, M.; Parker, G. Entrainment of Bed Sediment into Suspension. *J. Hydraul. Eng.* **1991**, *117*, 414–435. [CrossRef]

41. Verney, R.; Deloffre, J.; Brun-Cottan, J.-C.; Lafite, R. The effect of wave-induced turbulence on intertidal mudflats: Impact of boat traffic and wind. *Cont. Shelf Res.* **2007**, *27*, 594–612. [CrossRef]

42. Hawley, N.; Harris, C.K.; Lesht, B.M.; Clites, A.H. Sensitivity of a sediment transport model for Lake Michigan. *J. Great Lakes Res.* **2009**, *35*, 560–576. [CrossRef]

43. Matty, J.M.; Anderson, J.B.; Dunbar, R.B. Suspended sediment transport, sedimentation, and resuspension in Lake Houston, Texas: Implications for water quality. *Environ. Geol. Water Sci.* **1987**, *10*, 175–186. [CrossRef]

44. Gao, J.H.; Jia, J.; Kettner, A.J.; Xing, F.; Wang, Y.P.; Xu, X.N.; Yang, Y.; Zou, X.Q.; Gao, S.; Qi, S.; et al. Changes in water and sediment exchange between the Changjiang River and Poyang Lake under natural and anthropogenic conditions, China. *Sci. Total Environ.* **2014**, *481*, 542–553. [CrossRef]

45. Zhang, S.; Liu, Y.; Yang, Y.; Sun, C.; Li, F. Erosion and deposition within Poyang Lake: Evidence from a decade of satellite data. *J. Great Lakes Res.* **2016**, *42*, 364–374. [CrossRef]

46. Wang, H.; Kaisam, J.P.; Liang, D.; Deng, Y.; Shen, Y. Wind impacts on suspended sediment transport in the largest freshwater lake of China. *Hydrol. Res.* **2020**, *51*, 815–832. [CrossRef]

47. Luettich, R.A.; Harleman, D.R.F.; Somlyódy, L. Dynamic behavior of suspended sediment concentrations in a shallow lake perturbed by episodic wind events. *Limnol. Oceanogr.* **1990**, *35*, 1050–1067. [CrossRef]

48. Mei, C.C.; Fan, S.; Jin, K. Resuspension and transport of fine sediments by waves. *J. Geophys. Res.* **1997**, *102*, 15807–15821. [CrossRef]

49. Sanford, L.P.; Halka, J.P. Assessing the paradigm of mutually exclusive erosion and deposition of mud, with examples from upper Chesapeake Bay. *Mar. Geol.* **1993**, *114*, 37–57. [CrossRef]

50. Soulsby, R.L. *Dynamics of Marine Sands: A Manual for Practical Applications*; Thomas Telford Publishing: London, UK, 1997.

51. L'Agence Nationale de Protection de l'Environnement (ANPE). *Rapport sur le Suivi Scientifique au Parc National de L'ichkeul Annee 2006–2007*; ANPE: Tunis, Tunisia, 2008.